UDC 538.975 DOI: 10.18698/1812-3368-2022-1-122-140

NON-STATIONARITY EFFECTS IN POLYMER MEMBRANE SWELLING AS STUDIED BY INFRARED FOURIER SPECTROMETRY TECHNIQUE

N.F. Bunkin[1, 2] nbunkin@kapella.gpi.ru
S.V. Bashkin[1] bashkinv@bmstu.ru
S.V. Gudkov[2, 3] s_makariy@rambler.ru
M.S. Kiryanova[1] marykrnv@bk.ru
V.A. Kozlov[1, 2] vkozlov@bmstu.ru

[1] **Bauman Moscow State Technical University, Moscow, Russian Federation**
[2] **Prokhorov General Physics Institute, Russian Academy of Sciences, Moscow, Russian Federation**
[3] **Lobachevsky University, Nizhny Novgorod, Russian Federation**

Abstract

Nafion polymer membrane swelling mode in water poured into a cuvette, the cuvette characteristic size of the order of the membrane thickness, was investigated experimentally using the infrared Fourier spectrometry. Interest in these studies is based on the fact that, when a *Nafion* membrane is swelling in a cuvette sized much larger than the membrane thickness, polymer fibers are effectively unwinding into the water volume. However, this process was not studied in the case, where the area that could be occupied by the unwound polymer is limited by the cuvette size. It was shown that temporal dynamics of the polymer transition from a hydrophobic state to the hydrophilic state had several specific features depending on the cuvette size, isotopic composition, ion content and water pretreatment. It was suggested that dynamics of the cavity formation and collapse should be influenced by the dissolved gas nanobubbles. Indeed, the investigated liquid samples were not degassed. When polymer fibers are unwound, protrusions and irregularities appear on the hydrophobic membrane surface playing the role of nucleation centers for the surface nanobubbles. These nanobubbles are "carried away" by the growing fibers towards the cuvette window, and coalescence (collapse) of the nanobubbles could occur in the area of arising mechanical stresses, which should contribute to formation of a cavity. This is indirectly confirmed by results obtained in this work

Keywords

Infrared Fourier transform spectrometry, transmittance, polymer membranes, hydrophobicity, hydrophilicity

Received 09.04.2021
Accepted 11.05.2021

This work was supported by a grant from the President of the Russian Federation to support young Russian scientists (MD-2128.2020.11)

Introduction. Recently, the *Nafion* polymer membranes (*DuPont Nafion*™) are being rather intensively studied, see, for example, [1]. Interest in these studies is associated with the use of *Nafion* membrane in the low-temperature hydrogen cells [2, 3]. As a rule, most experimental works are studying the polymer internal structure. At the same time, certain works investigated properties of the water layers adjacent to the polymer membrane surface. Thus, work [4] described experiments, where it was found that, when a *Nafion* membrane is immersed in an aqueous suspension of colloidal microspheres, they are repelled from the membrane at a distance of several hundred microns. The area, from which colloidal microspheres are effectively pushed out, is called the exclusion zone.

Experiments described below were significantly motivated by previous research in photoluminescence spectroscopy [5–7]. Following the experiment results, distribution of the *Nafion* $N_{Naf}(x)$ membrane particles' density in the water volume was found. As shown in [7], when the *Nafion* membrane plane-parallel plate 175 μm thick was swelling in water (the cuvette volume with water, where the membrane swelled, was much larger than the plate volume), wide Gaussian distribution with the $N_{Naf}(x)$ particles' density appeared in the water volume centered on the membrane surface. This means that membrane particles in the water volume were not getting off the membrane surface, i.e., stationary density gradient of the *Nafion* $N_{Naf}(x)$ membrane particles appeared in the liquid. It was formation of a stationary gradient with the $N_{Naf}(x)$ density that was called in [7] the effect of "sprouting" ("unwinding") polymer fibers into the liquid volume. Dependence obtained in [7] is shown in Fig. 1. The figure presents the X_0 half-width of the $N_{Naf}(x)$ Gaussian distribution depending on the

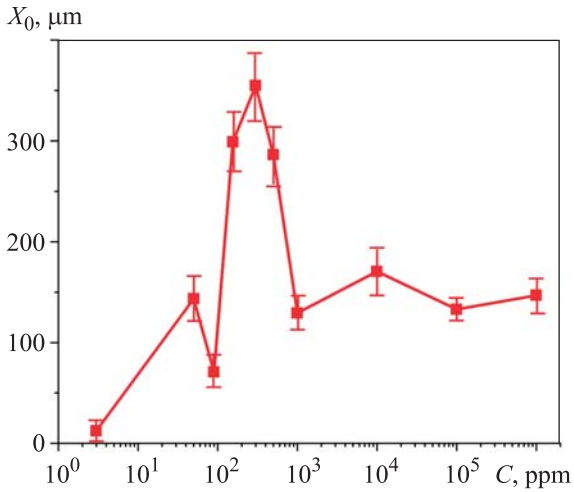

Fig. 1. Dependence of the X_0 size alteration in the area filled with unwinding polymer fibers on the deuterium content [7]

deuterium content in water, where the polymer was swelling; the deuterium content in the samples was changing as a result of bulk mixing of heavy water (deuterium content 10^6 ppm), deuterium depleted water (DDW, deuterium content 3 ppm) and ordinary natural water (deuterium content 157 ± 1 ppm, see [8]). According to the dependence, the X_0 value depends nonmonotonically on the deuterium content. The first point in this dependence corresponds to the deuterium depleted water; the unwinding effect is missing in DDW.

The question arises: what would happen, if the *Nafion* membrane plate is inside the cuvette with liquid, and the L distance between the cuvette windows is less than X_0? In accordance with data shown in Fig. 1, the effect of polymer fibers unwinding in the deuterium-depleted water was not found; in this case, $X_0 \approx 0$ within the experimental error, i.e., there should be no peculiarities. However, if $L < X_0$, then it should be expected that the *Nafion* membrane sprouting would rest against the cuvette windows, and the membrane would swell under conditions different from those introduced in a cuvette with a volume substantially larger than the polymer membrane volume.

In addition, the *Nafion* membrane has hydrophobic properties, i.e., the water drop contact angle on the membrane surface is close to 90°. However, as it swells in water, the membrane becomes hydrophilic; then the contact angle becomes significantly lower than 90°. Photographs illustrating transition dynamics of the 175-μm-thick *Nafion* membrane plate from hydrophobic state to the hydrophilic state are provided in Fig. 2. Hydrophobic properties of the *Nafion* membrane were monitored visually by changing the contact angle. Further, the plate was placed in water for 10 min, then it was removed from water, and a drop of water was again applied to it. The contact angle was not changed for 190 min,

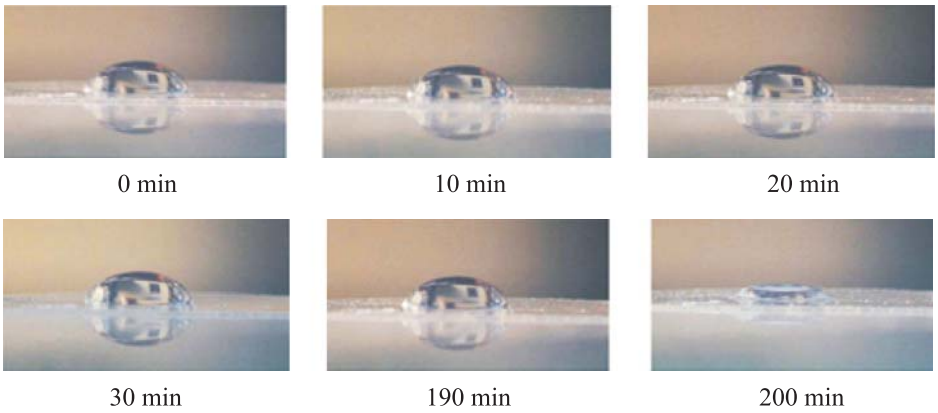

Fig. 2. *Nafion* membrane transition dynamics from a hydrophobic state to the hydrophilic state (sharp alteration in the contact angle is observed at the 200th minute)

i.e., the polymer retained its hydrophobic properties, but at the 200th minute the contact angle changed abruptly; the membrane became hydrophilic.

Work objective is to experimentally study temporal dynamics of the polymer fibers unwinding and transition from a hydrophobic state to the hydrophilic state using the infrared (IR) Fourier transfer spectrometry.

Materials and methods. Experiments were carried out on the FSM-2201 analytical Fourier spectrometer (*Infraspec LLC*, Russia, St. Petersburg). Spectrometer characteristics, cm^{-1}: spectral range 370–7800; spectral resolution in the entire range 1.0; absolute error in the entire range ± 0.05.

In the IR Fourier transform spectrometry, the 1.8–2.2 μm spectral range was investigated. Selection of the range is due to the following. The highest absorption in water is realized in the stretching vibration band in the 2.7–3.3 μm range. For a *Nafion* membrane plate 175 μm thick, transmittance in this range isclose to zero. At the same time, absorption near 2 μm is not so high and is caused by a combination of asymmetric stretching and flexural vibrations of the water molecule [9]. The moment the liquid was poured into the cuvette corresponded to the time reference. Transmittance of a cuvette with water containing the membrane plate was measured in the experiments. Each measurement consisted of 15 successive records of the transmittance followed by averaging for 40 s (taking into account the background absorption subtraction due to the air humidity). Time interval between separate measurements was 5 min. The experimental protocol is described in detail in [10, 11], where the *Nafion* membrane swelling in water with different deuterium content was studied experimentally using the IR Fourier transform spectrometry.

Nafion N117 membrane plate (*Sigma Aldrich*, USA) with thickness of L_0 = = 175 μm and area of 1×1 cm^2 was used in the experiments. The plate was placed in a cuvette with CaF_2 windows. This material is transparent to infrared radiation in a wide spectral range (the long-wavelength transparency limit corresponds to the wavelength of $\lambda = 3$ μm). In the case under consideration, the quality of window polishing was very important: characteristic roughness of the window surface was 2.5–5.0 μm. Before each experiment, the windows were rinsed with water cleared according to the *Milli-Q* technology, then they were dried while removing dust (stream of chemically pure nitrogen). The L distance between the windows (cuvette thickness) was varying with a step of 10 μm in the 180–220 μm range. The following types of water were studied: *Milli-Q* with resistivity of 18 MΩ (measured after receiving the sample) and deuterium content of 157 ± 1 ppm; deuterium depleted water (DDW, *Aldrich*, USA, deuterium content 3 ppm); NaCl solutions prepared on the basis of *Milli-Q* water for concentra-

tions in the range of $1–10^{-14}$ M; *Milli-Q* water vigorously shaken using the *Multi Speed Vortex MSV-3500* platform at the 20 Hz frequency for 1 min. Interest in studying the aqueous solutions of salts is due to the fact that ionic additives lead to an increase in bulk density of the ion-stabilized nanobubbles [12–14]. Selection of the 10^{-14} M concentration value was motivated by results given in [15], where mobility of the *Spirostoma ambiquum* ciliate in the NaCl aqueous solutions at various concentrations was studied. At the specified NaCl concentration, ciliate mobility was minimal, i.e., it approached zero. Interest in studies of water and aqueous solutions subjected to intense shaking is following results published in [16, 17]. As shown in these works, vigorous shaking causes a significant increase in the gas nanobubbles bulk density.

Features of the cuvette used in the experiments. A cuvette filled with water is shown in Fig. 3. The diagram of formation of a cavity free from water particles, when the cuvette is filled with natural water, and the absence of this cavity, when the cuvette is filled with deuterium-depleted water (DDW), is provided in Fig. 3, *a*. The cavity free from liquid is clearly visible in the photograph of the cuvette after filling with ordinary water (Fig. 3, *b*). In the photograph of the cuvette after filling with deuterium-depleted water (Fig. 3, *c*), the cavity is missing. It is very important that the volume of liquid poured into the cell always should exceed the cell volume, i.e., if the liquid enters one of the inlets (arrows in Fig. 3, *a*, circles in Fig. 3, *b* and *c*), then the water should come out from another opening. With this filling, no gas bubbles are formed inside the liquid, and the entire cuvette volume (except for the cavity) is uniformly filled with water. Thus, the cavity formed when pouring ordinary water could appear only as a result of contact between the *Nafion* hydrophobic membrane surface and the water molecules. After filling, the cuvette inlet and outlet openings were closed with *Teflon* inserts. In this case, tightness was missing, i.e., air could penetrate into the cuvette during the experiment. According to the model below, the cavity is formed as a result of water particles contact with the membrane surface and of the instantaneous unwinding of hydrophobic polymer fibers into the liquid volume. Since the X_0 area size occupied by the unwound polymer fibers in the cuvette significantly exceeds the size of the *Nafion* membrane plate and is much lower than the L distance between the cuvette windows, the polymer fibers would forcefully abut against the cuvette windows. This would lead to emergence of a field of local shear stresses and “squeezing out” water molecules trapped between the hydrophobic fibers. At the same time, peripheral areas of the *Nafion* membrane plate (see Fig. 3, *a*) are always in contact with water, and polymer in the peripheral areas continues to swel

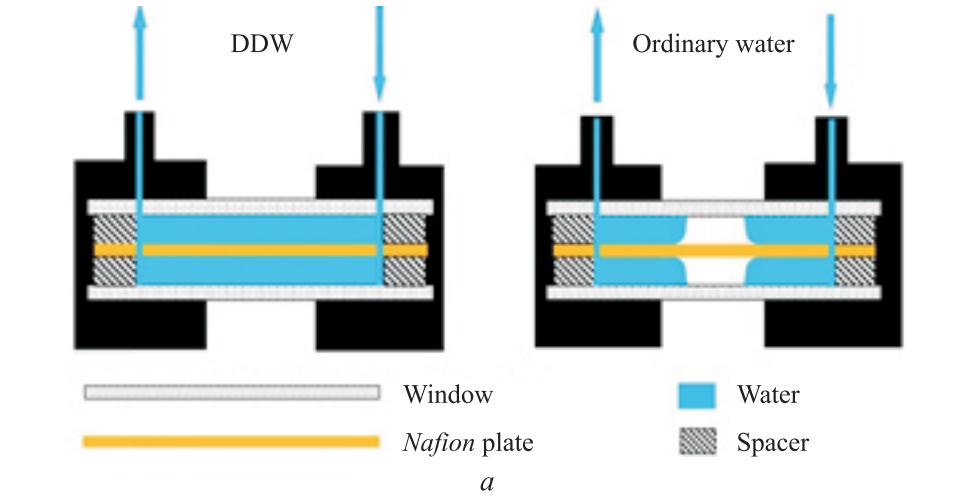

a

b

c

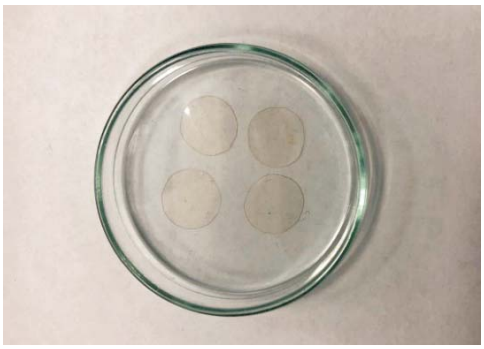

d

Fig. 3. Cell used in experiments in IR Fourier transform spectrometry:
a is layout of a cell filled with deuterium-depleted water and ordinary water; photographs: *b* are cells after filling with ordinary water; *c* are cells after filling with deuterium-depleted water; *d* is *Nafion* membrane plates (distance between the windows L = 200 μm)

despite the cavity presence. Thus, as a result of contact with water in the peripheral areas, the unwound fibers lose their hydrophobic properties, and the cavity collapses. The collapse rate should depend on the area of water contact with the plate peripheral regions, as well as on the surface roughness degree of the fluorite windows, since the cavity collapse kinetics is controlled by friction forces

between the unwound fibers and the cuvette window surface. Therefore, the plates in the case under consideration had the same shape and size (Fig. 3, *d*). In addition, the quality of window polishing is an uncontrollable parameter, so the cuvette was assembled in such a way that window surfaces in contact with the liquid were the same.

Missing cavity in the case of deuterium-depleted water, in contrast to ordinary water, could be explained within the frames of approach proposed in [7] (see Fig. 1). Since the water size area occupied by the polymer fibers is $X_0 \approx 300$ μm, and the *Nafion* membrane plate thickness is $L_0 = 175$ μm, for ordinary water the size of the area occupied by unwound polymer fibers is about 12 μm on each side of the plate. In this regard, the unwound polymer fibers in ordinary water rest against the cuvette windows. Consequently, creation of the local shear stresses field is stated, which leads to "intensification" of the hydrophobic effect: due to local stresses arising from the polymer fibers contact with the cuvette window surface, water molecules are most effectively pushed out of the gaps between hydrophobic fibers causing formation of a cavity. Micro-rheological properties of polymer fibers are manifested in water (soft matter micro-rheological properties are described in more detail in [18]).

Experiment results. In the experiments, values were measured of the transmission coefficient $K = I/I_0$, where I, I_0 are the transmitted and incident radiation intensities, which, according to the Lambert — Bouguer — Beer law [19], are related by relation $I = I_0 \exp(-\kappa L)$, κ is the extinction coefficient, L is the distance between the cuvette windows. Typical example of the transmission spectrum for ordinary water (deuterium content 157 ppm) poured into a cuvette with $L = 180$ μm in the range of $\lambda = 1.8$–2.2 μm, is shown in Fig. 4.

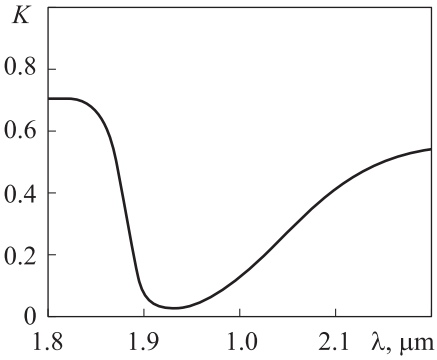

Fig. 4. Water transmission spectrum in the $\lambda = 1.8$–2.2 μm range (distance between the windows $L = 180$ μm)

Spectral minimum is realized at $\lambda = 1.93$ μm. It is noted that at the t swelling time and the L distance small values for all spectrograms transmittance $K\big|_{\lambda=1.8\ \mu m} \approx 0.7$, decreases slightly with the t and L increasing values, while at $\lambda = 2.2$ μm, the value decreases more. Decrease in K at the edges of the band under study is associated with additive contribution of the more intense absorption band centered near $\lambda = 3.0$ μm. This band is caused by stretching vibrations of water molecules [9]. Since primarily the $\left|\ln K_{\min}\right|$ is of in-

terest at the wavelength of λ = 1.93 μm, it is advisable to count the $K_{\min}$ from the value common to all spectrograms. Indeed, the logarithm at $K_{\min} < 1$ rapidly decreases, and inaccuracies in determining the $K_{\min}$ could lead to significant errors in determining the $\left|\ln K_{\min}\right|$. Therefore, for all spectrograms presented below, $K\big|_{\lambda = 1.8\ \mu\text{m}} = 0.7$.

$\left|\ln K_{\min}\right|$ value measurement results for water in a cuvette depending on the distance between the fluorite windows (L = = 180, 190, 200, 210, and 220 μm) are shown in Fig. 5. Dependencies are the result of averaging over five successive measurements. Selection of the minimum value L = 180 μm is due to the fact that thickness of the *Nafion* N117 membrane plate is L_0 = = 175 μm ≈ 180 μm; selection of the L = 220 μm maximum value — that the I intensity of transmitted radiation actually reaches the zero level, i.e., measurement results are incorrect. The $\left|\ln K_{\min}\right|(L)$ dependence obtained for water (see Fig. 5) is approximated by function $Y = 0.027 + 0.019X$, i.e., for κ ≈ 0.019 μm^{-1}. The $\left|\ln K_{\min}\right|$ value was measured for a dry (anhydrous) *Nafion* membrane. In this case, absorption at the λ = = 1.93 μm wavelength is due to water encapsulated inside the nanometer-sized closed cavities of a dry membrane [1]: $\left|\ln K_{\min}\right| = \kappa \left(C_w\right)_0 L_0$, where $\left(C_w\right)_0$ is water concentration inside the dry *Nafion* membrane. The following estimate is received: $\left(C_w\right)_0 = 0.174$.

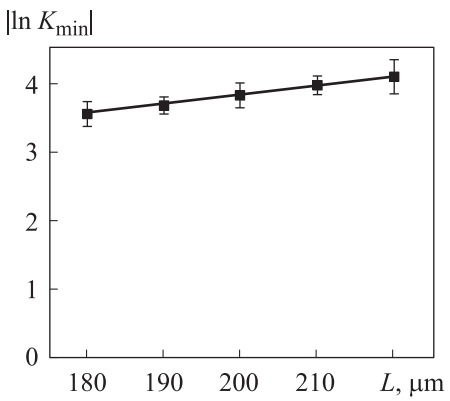

Fig. 5. $\left|\ln K_{\min}\right|(L)$ dependencies

Transmission spectra of the *Nafion* membrane, which was soaked in various liquids, were recorded with an interval of 5 min. Typical transmission spectra taken with an interval of 5 min at a time interval t = 70–100 min in ordinary water in a cuvette with a distance of L = 200 μm are shown in Fig. 6. The transmittance gradually decreases as it swells.

Transmittance dependences for deuterium-depleted water (deuterium content 3 ppm) in a cuvette with a distance of L = 200 μm in the interval t = 0–25 min are presented in Fig. 7. Here t = 0 corresponds to the time of pouring the liquid sample into a cuvette and taking the first measurement, which takes about 15 s, i.e., the first point on this graph corresponds to the t ≈ 30 s time. The spectra are practically identical for all the t values. Transmission spectrum is provided here for ordinary water taken at the t ≈ 30 s

time, which differs significantly from the corresponding spectra for the deuterium-depleted water. Let us note that [11] presents results of studying the water transmission spectra in the range of 1.8–2.2 μm depending on the C deuterium content: the K transmittance is the same in the range of C = = 1–10^4 ppm, i.e., the identified effect could not be associated with different absorption characteristics of ordinary and deuterium-depleted water. It could be possible that difference in spectra (see Fig. 7) is associated with the absence of polymer fibers unwinding in deuterium-depleted water and, accordingly, with the missing cavity in it.

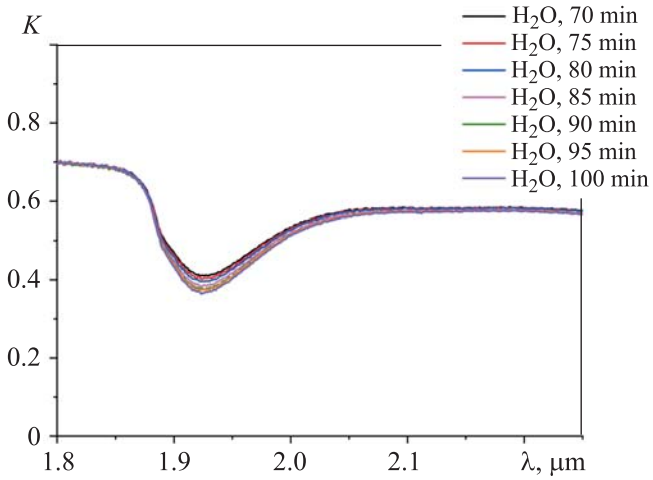

Fig. 6. Spectra of the K transmittance in the λ = 1.8–2.2 μm range, when soaking the *Nafion* membrane in ordinary water (deuterium content 157 ppm) for 70, 75, 80, 85, 90, 95 and 100 min

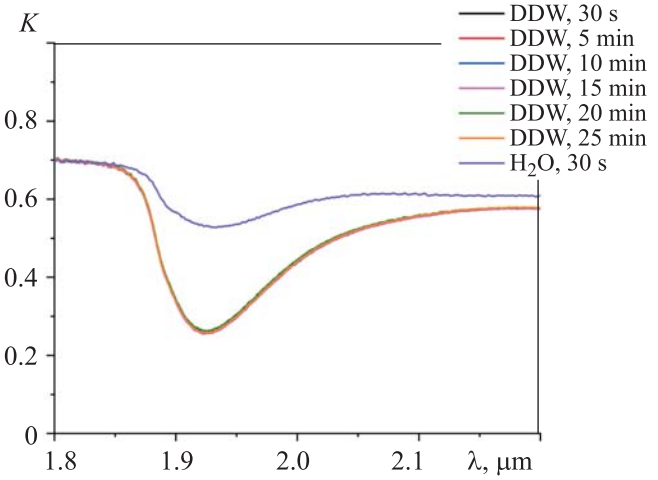

Fig. 7. Transmittance spectra in the range of λ = 1.8–2.2 μm, when placing the *Nafion* membrane plate in a cuvette with deuterium-depleted water

Based on the obtained spectra, it is possible to estimate the $\langle C_w \rangle$ water concentration averaged over the L cuvette length. By rewriting the Bouguer's law in the form:

$$I(t) = I_0 \exp\left(-\kappa \int_0^L C_w(t,x)dx \right) \approx I_0 \exp\left(-\kappa \langle C_w(t) \rangle L\right),$$

the following is obtained:

$$\langle C_w(t) \rangle = \frac{|\ln K_{\min}(t)|}{\kappa L}.$$

The formula takes into account dependence $\langle C_w \rangle$ on the t soaking time as a parameter. Dependence $\langle C_w(t) \rangle$ for cuvettes with a distances of L = = 180, 190, 200, 210, and 220 μm is shown in Fig. 8. The dashed line corresponds to water concentration of water in the dry *Nafion* membrane (baseline).

Let us consider (for definiteness) dependence $\langle C_w(t) \rangle$ for L = 180 μm. Water concentration undergoes a sharp increase after about 10 min of swelling, which is accompanied by the cavity collapse (see Fig. 3, *a*). Let us call this dramatic alteration as the first jump. Then, another jump occurs at about 90 min of swelling, which is not associated with the cavity collapse (highlighted in blue), i.e., the second jump. Note that second jumps, only with a smaller amplitude, are also observed at the distances of L = 190, 210, and 220 μm (highlighted by corresponding colors).

Measurements demonstrated that the first jump was associated with the cavity collapse. In this case, the polymer surface is covered with liquid, which corresponds to the normal swelling mode. Thus, the second jump could be associated only with a rather sharp increase in water concentration in the membrane volume. To test this hypothesis, water concentration time course was investigated in the membrane volume during its drying:

$$\langle C_w(t) \rangle_0 = \frac{|\ln K_{\min}(t)|}{\kappa L_0}.$$

Here L_0 = 175 μm is the plate thickness. The membrane in this experiment was soaked in a cuvette with a distance between the windows L = 180 μm for t_1 = 80 and t_2 = 110 min, i.e., before and after the second jump onset. Then the membrane was removed from the cuvette and dried in air at the room temperature (Fig. 9). Water concentration dependences $\langle C_w(t) \rangle_0$ on the drying time for the t_1 and t_2 swelling times are different. This indirectly confirms the hypothesis that the jump in dependence $\langle C_w(t) \rangle$ in Fig. 8 in the $t_1 < t < t_2$

interval is associated with structural alterations in the membrane volume, which are accompanied by a sharp increase in the water content. Note that the structural phase transitions that occur inside the polymer matrix upon swelling in water and are accompanied by a sharp increase in water content in the membrane volume are described, for example, in [20].

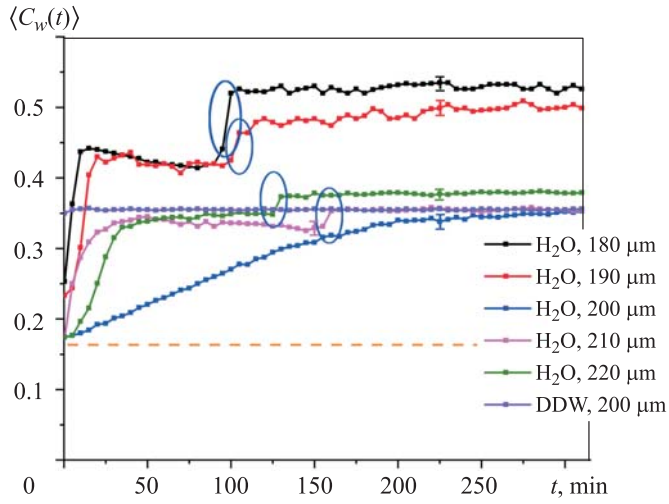

Fig. 8. Dependence of average water concentration $\langle C_w(t)\rangle$ at $180 \le L \le 220$ μm for ordinary water (deuterium content 157 ppm) and deuterium-depleted water (deuterium content 1 ppm), dashed line corresponds to water concentration of $C_{w0} = 0.174$ for a dry *Nafion* membrane

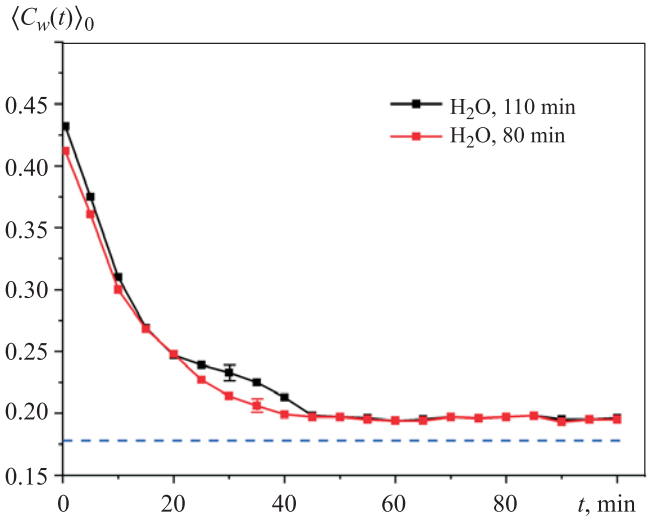

Fig. 9. Dependence of the average water concentration $\langle C_w(t)\rangle_0$ on the t drying time of the *Nafion* membrane after soaking in a cuvette with a distance between the windows of L = 180 μm for 80 and 110 min, dashed line corresponds to the $C_{w0} = 0.174$ water concentration for a dry *Nafion* membrane

Let us get back to Fig. 2, which shows the Nafion membrane transition from the hydrophobic state to the hydrophilic state, when the *Nafion* N117 membrane plate (plate thickness 175 μm) is soaked in ordinary natural water (deuterium content 157 ppm) in a cuvette with unlimited volume (Petri dish). In this case, transition to the hydrophilic state occurs much earlier than when a membrane swells in the Petri dish. This hypothesis is also supported by dependences $\langle C_w(t) \rangle$ for cuvettes with the $L = 190$, 210, and 220 μm thicknesses. The second jump in such cuvettes also occurs much earlier than transition to the hydrophilic state, when polymer membrane swells in the Petri dish (see Fig. 2). Thus, the effect of polymer fiber sprouting affects the membrane swelling kinetics: the weaker this effect is expressed, the faster transition to the hydrophilic state occurs. Research in this direction continues, and this conclusion would be further refined.

Kinetics of transition to the hydrophilic state is also affected by isotopic composition of water, where the membrane swells (see Fig. 8). As follows from dependence $\langle C_w(t) \rangle$, no features for deuterium-depleted water (distance between the cuvette windows is L = 200 μm) in the form of the first and second jumps are present. A cavity (see Fig. 3, *a*) for deuterium-depleted water is not being formed; there is also no jump associated, according to the hypothesis, with structural alterations in the membrane volume. A separate work would be devoted to a more detailed study of the water swelling dynamics with different isotopic compositions (in particular, studying the second jump appearance).

Let us pay attention to another interesting feature that is manifested during swelling of the *Nafion* N117 membrane plate with thickness of L_0 = 175 μm in ordinary water (deuterium content 157 ± 1 ppm) in a cuvette with a distance between the windows of L = 200 μm (see Fig. 8). In this case, a cavity free of water particles appears and does not disappear up to $t \sim 200$ min. The question arises, why does the cavity collapse in the cell with the distance between the windows of L = 200 μm occur so slowly? Membrane fibers unwound in the water volume could occupy an area of (200 – 175)/2 ≈ 12 μm on both sides of the plate. In this case, the cavity collapses abnormally slowly. However, it was not established, why this size affects the membrane polymer fibers in such a way.

Let us consider a case, where L = 200 μm, in more detail. Dependences of water $\langle C_w(t) \rangle$ in a cuvette, which windows are oriented so that surfaces of the liquid sample and CaF_2 are fixed, are shown in Fig. 10. Dependences are consistent with samples from different *Milli-Q* units on different days. Within 100 min, it makes no sense to calculate the experimental errors, as during this time period, points on the curves actually coincide, and only at $t > 100$ min

the spread between the extreme points exceeds 1 % in concentration $\langle C_w(t) \rangle$. In this regard, Fig. 9 shows the errors for times $t > 100$ min; these errors are calculated from the results of five consecutive measurements.

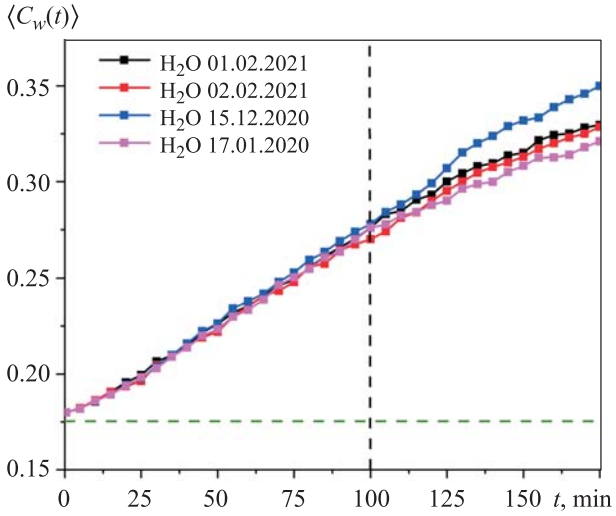

Fig. 10. Dependence of average water concentration $\langle C_w(t) \rangle$ at $L = 200$ μm for ordinary water obtained on various *Milli-Q* units (dashed line corresponds to water concentration of $C_{w0} = 0.174$ for a dry *Nafion* membrane)

Membrane fibers abut against the window surface; therefore, collapse dynamics of the cavity shown in Fig. 3, *a* could be controlled by interaction between the unwound fibers and the window surface. Apparently, it is possible to assert in this case a specific frictional force. Typical examples of dependencies $\langle C_w(t) \rangle$ for two different cuvettes are presented in Fig. 11: the straight-line relationship remains within 100 minutes of swelling, but for one straight line the slope coefficient is $k = 0.00126$, and for the other $k = 0.00111$. Since the cuvette windows were purchased from one and the same manufacturer and were not subjected to special treatment, the only explanation for different dependences slope shown in Fig. 11, is the different degree of roughness of the window surface. It is possible that for more rough surfaces the cavity collapse rate would be lower, i.e., $k = 0.00111$. Relationship between the collapse rate and the roughness degree is apparently caused by the fact that nanometer gas bubbles filled with dissolved air are formed on tips and rough regions of a solid substrate (see [12] and the cited references), which should contribute to formation of a cavity created by hydrophobic fibers. For more detailed analysis, it is necessary to carry out experiments, where the fluorite surface would be modified by adding hydrophobic or hydrophilic properties. In this work, all results are presented for a cuvette with $k = 0.00111$.

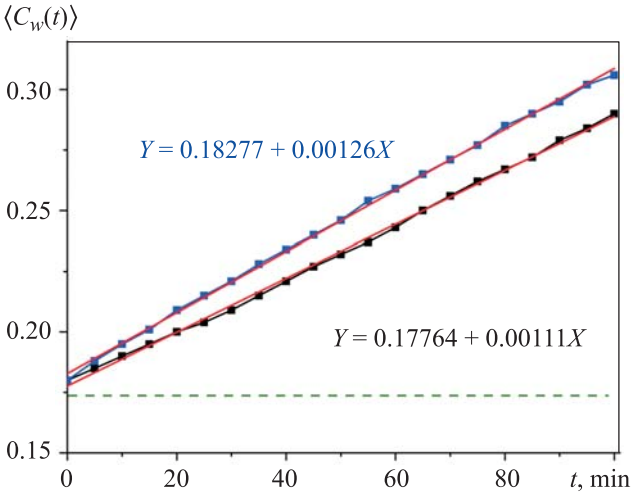

Fig. 11. Dependence of average water concentration $\langle C_w(t) \rangle$ for ordinary water obtained in two different cuvettes with a distance between the windows of L = 200 μm (dashed line corresponds to water concentration $C_{w0} = 0.174$ for a dry *Nafion* membrane)

It turned out that collapse dynamics of a cavity formed by hydrophobic polymer fibers depends not only on the surface quality of cuvette windows, but also on the ionic composition and pretreatment of the liquid samples. Thus, Fig. 12 presents a family of dependences $\langle C_w(t) \rangle$ for the NaCl aqueous solution, which concentration varied in the range of 10^{-14}–1.0 M. As was noted before, the aqueous ion solutions study was motivated by works [12–14], where it was demonstrated that the nanobubbles volumetric density increased with ion additions. For NaCl salt, the 10^{-14} M concentration is isolated. At this concentration, mobility of a certain class of ciliates has a deep minimum approaching almost zero [15]. In order not to clutter up Fig. 11, data is provided for concentrations of 1, 10^{-4}, 10^{-6} and 10^{-14} M, as well as dependence for water, estimates of the X_0 area size occupied by polymer fibers during their unwinding into a cuvette, which volume significantly exceeds the *Nafion* membrane plate volume. For this purpose, photoluminescence spectroscopy experiments were carried out described in [7]. According to the given dependences, the X_0 size is growing with an increase in the ion concentration, but at a concentration of less than 10^{-4} M, the X_0 value gets to the water level within the experimental error. At the same time, dependence $\langle C_w(t) \rangle$ differs from the straight-line to the 10^{-14} M concentration. The dependence is straightforward only for this concentration in the entire $0 < t < 100$ min area and practically coincides with

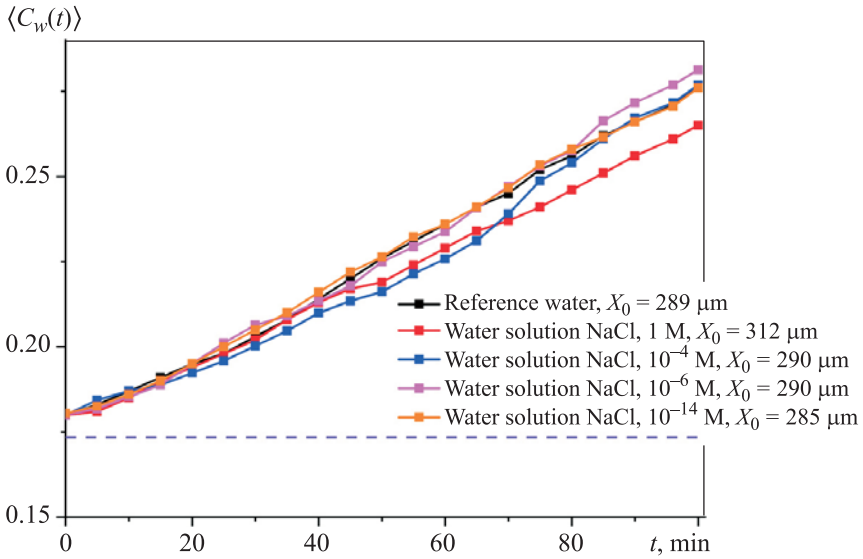

Fig. 12. Dependences $\langle C_w(t) \rangle$ for the NaCl aqueous solution with concentration of 1, 10^{-4}, 10^{-6} and 10^{-14} M at L = 200 μm, X_0 estimate (dashed line corresponds to the $C_{w0} = 0.174$ water concentration for a dry *Nafion* membrane)

dependence for water. Thus, deviations from the straight-line dependence could be associated with introduction of external ionic impurities into the water.

Samples of water were studied subjected to intense shaking on the *Vortex MSV-3500* vibration platform at the frequency of 20 Hz for 1 min. These studies were motivated by results presented in [16, 17], where it was shown that shaking led to an increase in the bulk density of nanobubbles by about 10 times. However, after shaking and settling for a certain time, the original properties should restore. Time dependence $\langle C_w(t) \rangle$ for the initial water before and after shaking, as well as for water settled for 1 day after shaking is shown in Fig. 13. Immediately after shaking and within 15 min, a slowdown in $\langle C_w(t) \rangle$ growth was observed in comparison with the initial water, and the X_0 size also increased. Liquid settled for 1 day returned to its original state. Thus, presence of nanobubbles, isotopic composition and dissolved ions affect hydrophobic properties of the polymer fibers that form the cavity (see Fig. 2).

Conclusion. Features of the cavity temporal dynamics shown in Fig. 2 are associated with the effect of polymer fibers growing into the water volume. This conclusion is based on the absence of this cavity in deuterium-depleted water, for which the sprouting effect is missing. If the L distance between the cuvette windows is less than the X_0 area, inside which the polymer fibers are growing in case of the cuvette "unlimited" size [11], then the polymer fibers sprouting into the wa-

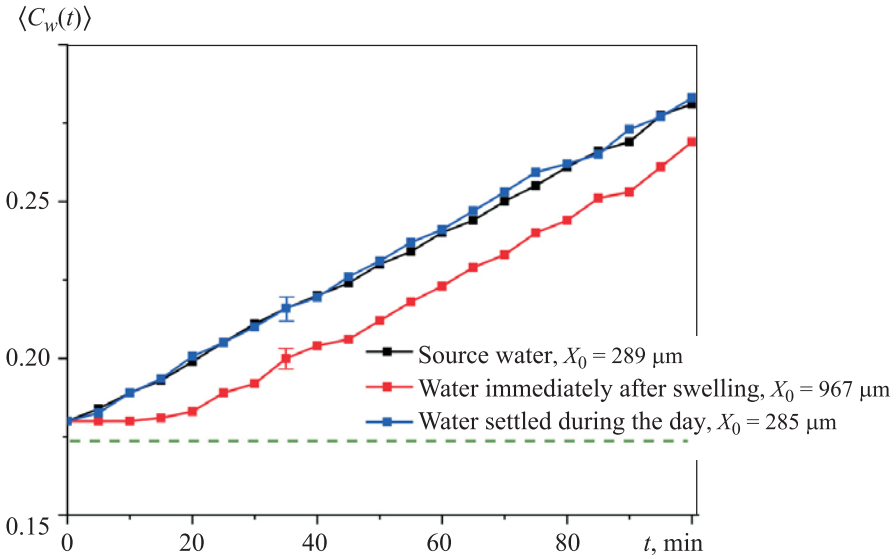

Fig. 13. Dependences $\langle C_w(t) \rangle$ for initial water (X_0 = 289 μm), water (X_0 = 967 μm) shaken on the vibration platform, and water (X_0 = 285 μm) settled for 1 day after shaking at L = 200 μm (dashed line corresponds to the $C_{w0} = 0.174$ water concentration for a dry *Nafion* membrane)

ter volume inevitably rest against the cuvette windows. This should lead to the appearing field of mechanical stresses and related deformations, i.e., microrheological properties of the swelling membrane are being manifested in the case under consideration [18]. It is important that these stresses arise in a system of "twisted" polymer fibers, which initially have hydrophobic properties, i.e., position of a water molecule in the intervals between such fibers would be unstable.

It should be expected that dynamics of the cavity formation and collapse should be influenced by dissolved gas nanobubbles. Indeed, the investigated liquid samples were not degassed. When polymer fibers were unwound, protrusions and irregularities appeared on the hydrophobic membrane surface playing the role of nucleation centers for the surface nanobubbles [12]. These nanobubbles were "carried away" by the germinating fibers towards the cuvette window, and coalescence (collapse) of nanobubbles could occur in the field of arising mechanical stresses, which should contribute to the cavity formation. This is indirectly confirmed by results obtained with the NaCl aqueous solutions, as well as with samples subjected to shaking. Indeed, as shown in [12–14], ion-stabilized gas nanobubbles with a radius of about 200 nm appear in aqueous solutions of salts in the liquid volume. Volumetric density of ion-stabilized gas nanobubbles in the deionized water (in this case, presence of the ionic component is due to intrinsic dissociation of the water molecules) was $n \sim 10^6$ cm^{-3}, i.e., there were

~ 10^3 nanobubbles between the membrane surface of ~ 1 cm^2 and the cell window. In this case, the n value depends on concentration of the C electrolyte as $C^{1/4}$ reaching a plateau $n \sim 10^8$ cm^{-3} at $C = 0.1$ M. It could be assumed that insignificant retardation of the cavity collapse is associated primarily with the increasing nanobubbles volumetric density (see Figs. 12 and 13). Apparently, the mechanism associated with nanobubbles should also be manifested for cuvettes, which windows have different roughness (see Fig. 12). Upon contact of a hydrophobic polymer fiber and a solid-state substrate, nanobubbles should be generated more efficiently on a rougher surface. Obviously, it is necessary to carry out experiments with degassed water for a more detailed analysis. However, the mechanism associated with the presence of nanobubbles could not be a key for forming a cavity, since there are only few nanobubbles. Thus, the main mechanism of cavity formation is precisely the hydrophobic properties of polymer fibers. Since the *Nafion* membrane plate in the peripheral areas contacts water (see Fig. 2), the unwound polymer fibers acquire hydrophilic properties over time, and as a result the cavity collapses.

REFERENCES

[1] Mauritz K.A., Moore R.B. State of understanding of Nafion. *Chem. Rev*., 2004, vol. 104, no. 10, pp. 4535–4586. DOI: https://doi.org/10.1021/cr0207123

[2] Liu L., Chen W., Li Y. An overview of the proton conductivity of Nafion membranes through a statistical analysis. *J. Membr. Sci*., 2016, vol. 504, pp. 1–9.
DOI: https://doi.org/10.1016/j.memsci.2015.12.065

[3] Wang Y., Chen K.S., Mishler J., et al. A review of polymer electrolyte membrane fuel cells: technology, applications, and needs on fundamental research. *Appl. Energy*., 2011, vol. 88, iss. 4, pp. 981–1007. DOI: https://doi.org/10.1016/j.apenergy.2010.09.030

[4] Pollack G.H. The fourth phase of water. Ebner and Sons, 2013.

[5] Ninham B.W., Lo Nostro P. Molecular forces and self assembly in colloid, nano sciences and biology. Cambridge Univ. Press, 2010.

[6] Bunkin N.F., Lyakhov G.A., Kozlov V.A., et al. Time dependence of the luminescence from a polymer membrane swollen in water: concentration and isotopic effects. *Phys. Wave Phen*., 2017, vol. 25, no. 4, pp. 259–271.
DOI: https://doi.org/10.3103/S1541308X17040045

[7] Bunkin N.F., Shkirin A.V., Kozlov V.A., et al. Near-surface structure of Nafion in deuterated water. *J. Chem. Phys*., 2018, vol. 149, iss. 16, art. 164901.
DOI: https://doi.org/10.1063/1.5042065

[8] Craig H. Standard reporting concentrations of Deuterium and Oxygen 18 in natural water. *Science*, 1961, vol. 133, no. 3467, pp. 1833–1834.
DOI: https://doi.org/10.1126/science.133.3467.1833

[9] Workman Jr.J., Weyer L. Practical guide and spectral atlas for interpretive near-infrared spectroscopy. CRC Press, 2013.

[10] Bunkin N.F., Balashov A.A., Shkirin A.V., et al. Investigation of deuterium substitution effects in a polymer membrane using IR Fourier spectrometry. *Opt. Spectrosc.*, 2018, vol. 125, no. 3, pp. 337–342. DOI: https://doi.org/10.1134/S0030400X18090072

[11] Bunkin N.F., Kozlov V.A., Shkirin A.V., et al. Dynamics of Nafion membrane swelling in H_2O/D_2O mixtures as studied using FTIR technique. *J. Chem. Phys.*, 2018, vol. 148, iss. 12, art. 124901. DOI: https://doi.org/10.1063/1.5022264

[12] Bunkin N.F., Bunkin F.V. Bubston structure of water and electrolyte aqueous solutions. *Phys.-Usp.*, 2016, vol. 59, no. 9, pp. 846–865.
DOI: https://doi.org/10.3367/UFNe.2016.05.037796

[13] Bunkin N.F., Shkirin A.V., Suyazov N.V., et al. Formation and dynamics of ion-stabilized gas nanobubble phase in the bulk of aqueous NaCl solutions. *J. Phys. Chem. B*, 2016, vol. 120, no. 7, pp. 1291–1303. DOI: https://doi.org/10.1021/acs.jpcb.5b11103

[14] Yurchenko S.O., Shkirin A.V., Ninham B.W., et al. Ion-specific and thermal effects in the stabilization of the gas nanobubble phase in bulk aqueous electrolyte solutions. *Langmuir*, 2016, vol. 32, iss. 43, pp. 11245–11255.
DOI: https://doi.org/10.1021/acs.langmuir.6b01644

[15] Lobyshev V.I., Tomkevich M.S., Petrushanko I.Yu. Experimental study of potentiated aqueous solutions. *Biophysics*, 2005, vol. 50, no. 3, pp. 416–420.

[16] Barkhudarov E.M., Kossyi I.A., Anpilov A.M., et al. New nanostructured carbon coating inhibits bacterial growth, but does not influence on animal cells. *Nanomaterials*, 2020, vol. 10, iss. 11, pp. 1–12.

[17] Bunkin N.F., Shkirin A.V., Ninham B.W., et al. Shaking-induced aggregation and flotation in immunoglobulin dispersions: differences between water and water–ethanol mixtures. *ACS Omega*, 2020, vol. 5, iss. 24, pp. 14689–14701.
DOI: https://doi.org/10.1021/acsomega.0c01444

[18] Furst E.M., Squires T.M. Microrheology. Oxford Univ. Press, 2017.

[19] Gebel G. Structural evolution of water swollen perfluorosulfonated ionomers from dry membrane to solution. *Polymer*, 2000, vol. 41, iss. 15, pp. 5829–5838.
DOI: https://doi.org/10.1016/S0032-3861(99)00770-3

[20] Alheshibri M., Qian J., Jehannin M., et al. A history of nanobubbles. *Langmuir*, 2016, vol. 32, iss. 43, pp. 11086–11100.
DOI: https://doi.org/10.1021/acs.langmuir.6b02489

Bunkin N.F. — Dr. Sc. (Eng.), Professor, Department of Physics, Bauman Moscow State Technical University (2-ya Baumanskaya ul. 5, str. 1, Moscow, 105005 Russian Federation); Leading Researcher, Prokhorov General Physics Institute, Russian Academy of Sciences (Vavilova ul. 38, Moscow, 119991 Russian Federation).

Bashkin S.V. — Senior Lecturer, Department of Physics, Bauman Moscow State Technical University (2-ya Baumanskaya ul. 5, str. 1, Moscow, 105005 Russian Federation).

Gudkov S.V. — Dr. Sc. (Biol.), Head of Biophotonics Center, Prokhorov General Physics Institute, Russian Academy of Sciences (Vavilova ul. 38, Moscow, 119991 Russian Federation); Professor, Lobachevsky University (Gagarina prospekt 23, Nizhny Novgorod, 603950 Russian Federation).

Kiryanova M.S. — Student, Department of Physics, Bauman Moscow State Technical University (2-ya Baumanskaya ul. 5, str. 1, Moscow, 105005 Russian Federation).

Kozlov V.A. — Cand. Sc. (Eng.), Assoc. Professor, Department of Physics, Bauman Moscow State Technical University (2-ya Baumanskaya ul. 5, str. 1, Moscow, 105005 Russian Federation); Leading Researcher, Prokhorov General Physics Institute, Russian Academy of Sciences (Vavilova ul. 38, Moscow, 119991 Russian Federation).

Please cite this article as:

Bunkin N.F., Bashkin S.V., Gudkov S.V., et al. Non-stationarity effects in polymer membrane swelling as studied by infrared Fourier spectrometry technique. *Herald of the Bauman Moscow State Technical University, Series Natural Sciences*, 2022, no. 1 (100), pp. 122–140. DOI: https://doi.org/10.18698/1812-3368-2022-1-122-140